



Improvement of Thermal Resistance of Surface-emitting Quantum Cascade Laser using Structural Function and 3D Thermal Flow Simulation

Shigeyuki Takagi¹, Hirotaka Tanimura¹^a, Tsutomu Kakuno², Rei Hashimoto², Kei Kaneko²
and Shinji Saito²^b

¹*Department of Electrical and Electronics Engineering, School of Engineering, Tokyo University of Technology,
1404-1 Katakura, Hachioji, Tokyo, Japan*

²*Corporate Manufacturing Engineering Center, Toshiba Corporation,
8 Shinisogo, Isogo, Yokohama, Kanagawa, Japan*

Keywords: Quantum Cascade Lasers, QCLs, Surface-emitting QCL, Photonic Crystal, PhC, Static Method, Structure Function, Thermal Resistance, Thermal Flow Analysis, Diamond Submount.

Abstract: We have evaluated the thermal resistance of the surface-emitting QCL, which is expected to increase the output and improve the beam quality, based on the structure function and 3D heat flow resolution. From the structure function, the thermal resistance of the surface emitting QCL was divided into the mesa for laser excitation, the InP substrate, and the CuW mount, and the total thermal resistance of 8.0 K/W was obtained. The thermal resistance obtained by the 3D thermal analysis simulation was estimated to be 8.3 K/W, which was in good agreement with that obtained from the structure function. Furthermore, the effect of the diamond submount was evaluated and it was shown that the thermal resistance was reduced to 5.2 K/W. It is considered that the thermal resistance is reduced by the horizontal transfer of heat in the diamond submount.


1 INTRODUCTION


A quantum cascade laser (QCL) is an n-type semiconductor laser that can obtain laser light in the infrared region (Faist et al., 1994). Since the oscillation wavelength of the QCL is in the infrared region called the fingerprint region of the molecule, many gases can be measured with high sensitivity. From the advantages, it is expected to be applied to trace substance detection and distant gas detection. In the detection of trace substances, the amount of laser light absorbed is measured, and it is necessary to propagate a long optical path length, and high output is desired. Further, in the distant gas detection, since the reflected light at the time of laser light propagation is detected, a high-power laser is required as a high-power laser, watt-class laser oscillation has been obtained by A. Evans et al. (Evans et al., 2007). This laser is an end face emitting type laser in which the directions of the laser

excitation and the laser emission coincide with each other. The laser beam is excited by concentrating the current in a narrow current path called a ridge. Therefore, the heat dissipation is low, and the laser beam is emitted from the narrow ridge into a wide space, so that there is a problem that the beam quality (M^2) is low.

On the other hand, a surface-emitting QCL that emits laser light in the vertical direction of the device using a photonic crystal (PhC) has been proposed (Colombelli, R., et al., 2003). By increasing the area of the excited part called a mesa, improvements in beam quality and heat dissipation can be expected. In the surface-emitting QCL using PhC, laser oscillation was reported by Colombelli et al. (Colombelli et al., 2003), and laser oscillation of 5 W was reported by Wang et al. (Wang et al., 2019).

One way to increase the output of the surface-emitting QCL is to improve heat dissipation. We determined the thermal resistance of the Au-

^a <https://orcid.org/0000-0002-7653-4602>

^b <https://orcid.org/0000-0002-1829-6482>

embedded type surface-emitting QCL from the structure functions obtained by the static method and the 3D thermal analysis simulation (Takagi et al., 2021). In this study, the thermal resistance of the InP-embedded surface-emitting QCL was estimated using these methods. Furthermore, as a method of increasing heat dissipation, we have proposed a method using a diamond submount. As a result of evaluation using 3D thermal analysis simulation, it was shown that the heat spreads horizontally in the diamond submount and the temperature rise of the mesa that excites the laser can be reduced to about 2/3.

2 SURFACE-EMITTING QCL

The structure of the surface-emitting QCL is shown in Fig. 1, where (a) is a cross-sectional view, (b) is a top view, and (c) is a bottom view. A mesa area where the input power is supplied and a dummy ridge are formed on an InP substrate with a thickness of 600 μm . In the mesa area, a photonic crystal (PhC) is formed on the active layer that excites the laser and PhC is embedded with InP. An Au electrode for current supply is formed on the opposite side of the InP substrate.

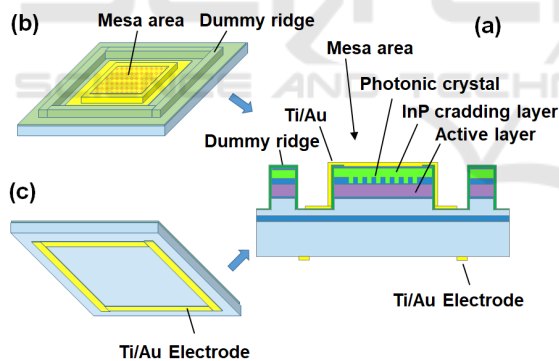


Figure 1: Surface emitting QCL, (a) Cross-sectional view, (b) top view, and (c) bottom view.

The surface-emitting device has an epi-side-down structure in which the mesa and dummy ridge sides are mounted on a CuW mount with AuSn solder. Figure 2 is an external photograph of the surface-emitting QCL used for the measurement, in which mesas and dummy ridges are observed to be formed on the InP substrate.

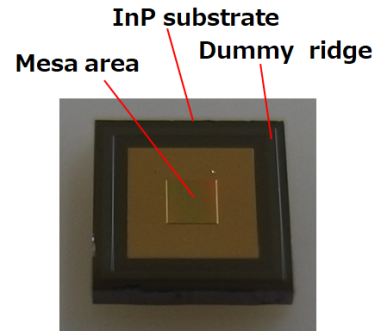


Figure 2: Photograph of surface-emitting QCL.

3 MEASUREMENT OF STRUCTURE FUNCTION

3.1 K-factor Measurement

We reported on a method for measuring the thermal resistance of end-face emitting QCLs using the static method (Takagi et al., 2019). In this paper, the static method was applied to the thermal resistance measurement of InP-embedded QCL. A T3Ster (Siemens AG) was used for the measurement. Since the resistance of a semiconductor device changes with temperature, the temperature change is proportional to the voltage change at the end of the device when a constant current is flowing. In the static method, this voltage change ΔT_{SP} [mV] is measured, and the device temperature change ΔT_j [K] is obtained using

$$\Delta T_j = K \cdot \Delta T_{SP}, \quad (1)$$

where K is a coefficient called K-factor.

The K-factor is required to measure the temperature of a surface-emitting QCL in the static method. Therefore, a surface-emitting QCL was installed in the thermostat of the T3Ster, the thermostat temperature was changed from 20 °C to 70 °C, and the K-factor was measured. The K-factor was determined to be -0.022772.

3.2 Structure Function

T3Ster was used to measure the structure function by the static method. The mounting part of the QCL mount was cooled to 20 °C, and the QCL device was heated by supplying about 1.6 W of electric power. After stopping the heating power supply, the QCL temperature during cooling was measured and the cooling curve was obtained. Assuming that the thermal resistances of each element constituting the

QCL is R_{th} and the heat capacity is C_{th} , the time constant τ during cooling is expressed by

$$\tau = C_{th} \cdot R_{th} . \quad (2)$$

The time constant τ was extracted from the inflection point of the cooling curve, and C_{th} and R_{th} were obtained from τ using Eq. (4). In the structure function, R_{th} is plotted on the horizontal axis and C_{th} is plotted on the vertical axis (Székely, 1997).

Fig. 3 shows the structure function of the surface emitting QCL. As shown in Fig. 1, the surface emitting QCL is divided into the mount, the InP substrate, and the mesa area. From the thermal conductivity and component size, it is estimated that the structure function divided by the inflection point corresponds to the three QCL components. In addition, the flat region with a thermal resistance over 8.5 K/W or more changes depending on whether the QCL is attached to a cooling plate. It is considered to be the thermal resistance between the surface emitting QCL and the T3Ster cooler, and the total thermal resistance of the surface emitting QCL is estimated to be about 8.0 K/W.

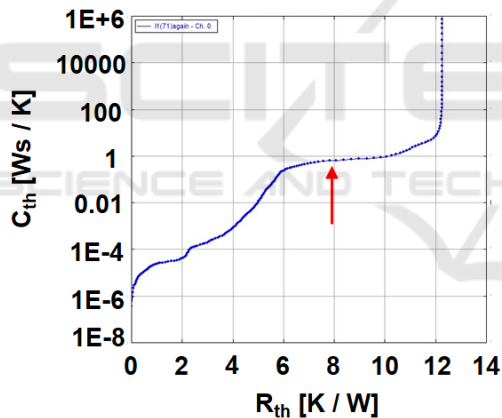


Figure 3: Structure function of surface emitting QCL.

4 THERMAL SIMULATION OF SURFACE-EMITTING QCL

4.1 3D Thermal Flow Simulation Model

As another method for analysing the thermal characteristics of the surface emitting QCL, thermal flow analysis using a 3D model was performed. A simulation model was constructed by inputting the 3D structure and physical property data of the surface emitting QCL. The thermal flow analysis software

STEAM (MSC software) and FloTHERM (Mentor Graphics Japan) were used as the simulator. The thermal flow analysis is performed using a natural convection model in which mesa area is overheated and natural convection is generated. The equation for gas flow is expressed by

$$\frac{\partial \rho}{\partial t} + \frac{\partial(\rho v_x)}{\partial x} + \frac{\partial(\rho v_y)}{\partial y} + \frac{\partial(\rho v_z)}{\partial z} = 0, \quad (3)$$

where ρ is the density, t is the time, and v_x , v_y , and v_z are the velocities in the x , y , and z directions, respectively. The heat equation is determined as

$$\frac{\partial u}{\partial t} = \frac{K}{\sigma \rho} \left(\frac{\partial^2 u}{\partial x^2} + \frac{\partial^2 u}{\partial y^2} + \frac{\partial^2 u}{\partial z^2} \right) + \frac{1}{\sigma} F(x, y, z, t), \quad (4)$$

where u is the temperature and is a function of the position and time. σ is the specific heat, and K is the thermal conductivity. F is the external heating value per time, and is a function of position and time.

The 3D structure of the surface-emitting QCL shown in Fig. 1 were input, and a three-dimensional model was constructed. Figure 4 (a) is a three-dimensional model of a surface-emitting QCL. The surface-emitting QCL has an epi-side-down structure in which the mesa area and dummy ridge sides are mounted on a CuW mount with AuSn solder. Fig. 4 (b) is a top view of the 3D model as in the photograph of Fig. 2. The outline of the InP substrate, mesa, dummy ridge, and Au electrode on the back surface are shown.

In the 3D model, the physical property values were as follows. The thermal conductivity of CuW mount, AuSn solder, InP, SiO₂, Ti, Au, Cu is 157, 59, 68, 1.38, 21, 296, 403 W/mK, respectively. For the PhC part in which InP was embedded, the thermal conductivity was calculated based on the volume ratio of the PhC and the InP. In the active layer, thin films of Al_{0.638}In_{0.362}As and Ga_{0.331}In_{0.669}As are alternately laminated. The thermal conductivity of the active layer was calculated by multiplying the film thickness ratio with InAlAs of 10.0 W/mK (Kim et al., 2002) and InGaAs of 5.6 W/mK (Adachi, 1985), and was estimated to be 7.5 W/mK. The temperature boundary condition is fixed at 0 °C on the mount with a cooling Peltier, and the ambient temperature of the surface emitting QCL is set at 25 °C.

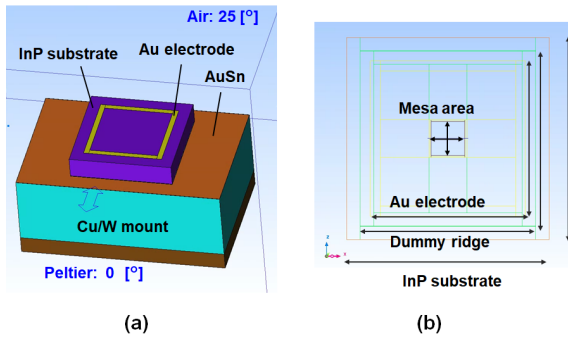


Figure 4: 3D simulation model of surface emitting QCL. (a) perspective view and (b) top view.

5 SIMULATION RESULTS

5.1 Thermal Resistance of Surface Emitting QCL

The temperature distribution of the surface emitting QCL was calculated under the conditions of the of 10 W input power to the mesa area. Figure 5 shows the temperature distribution of the surface-emitting QCL in the central cross section. The CuW mount has high thermal conductivity and the most of the mount is kept at 0 ° C. The temperature around the mesa area is higher than that in other parts. Since the temperature rise at an input power of 10 W is 82.63 ° C, the thermal resistance of the surface emitting QCL was calculated to be 8.3 K/W. This value was almost the same as the thermal resistance of 8.0 K/W obtained from the structure function. It shows the validity of the 3D thermal analysis simulation.

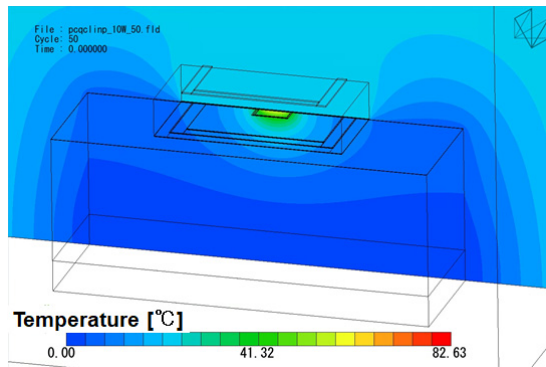


Figure 5: Temperature distribution of surface emitting QCL.

5.2 Effect of Diamond Submount

A diamond submount has a large value of 2000 W/mK, and it has been reported that the thermal resistance of light emitting device is reduced (Bezotosnyi et al., 2014). To reduce the thermal resistance of the surface emitting QCL, the thermal resistance of structure in which diamond was inserted between the substrate and the mount was evaluated by 3D thermal analysis simulation. Figure 6 is a 3D simulation model of a surface emitting QCL using a diamond submount. It is assumed that the lower surface of the diamond submount is soldered to CuW with AuSn having a thickness of 5 μm, and the InP substrate is soldered to the upper surface with AuSn having a thickness of 5 μm. The thermal conductivity of the diamond submount and AuSn was set to be 2000 W/mK and 59 W/mK in the calculation, respectively.

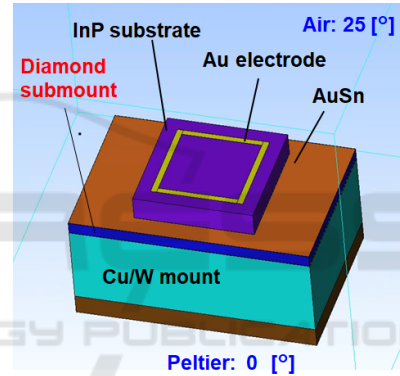


Figure 6: 3D simulation model of surface emitting QCL with diamond submount.

We applied the input power of 10 W to the mesa area of the QCL with diamond submount, and the temperature rise of the mesa area was calculated. Figure 7 (b) shows the simulation results. For comparison, Fig. 7 (a) shows the calculation results of the temperature distribution of the QCL without diamond submount. In the QCL with diamond submount (b), the temperature rise at an input power of 10 W was 52.47 ° C, and the thermal resistance was reduced to 5.2 K/W. Figure 8 shows the temperature rise of the mesa area when the power input is changed from 4 to 10 W. As the input power increases, the temperature difference with and without the diamond submount increases. It has been shown that the diamond submount is more effective under high input power operating conditions.

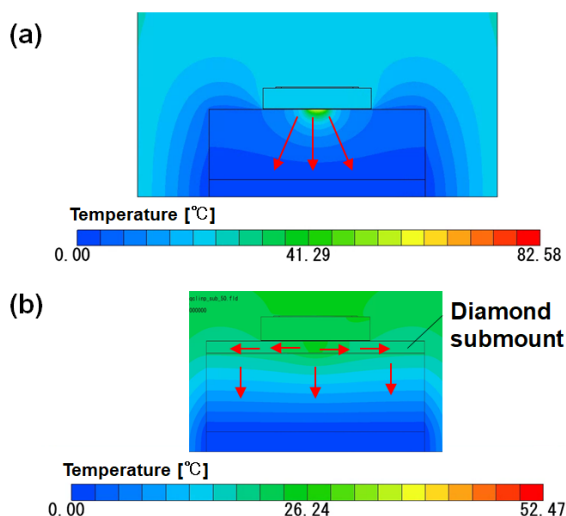


Figure 7: Comparison of temperature distribution between QCLs with and without diamond submount.

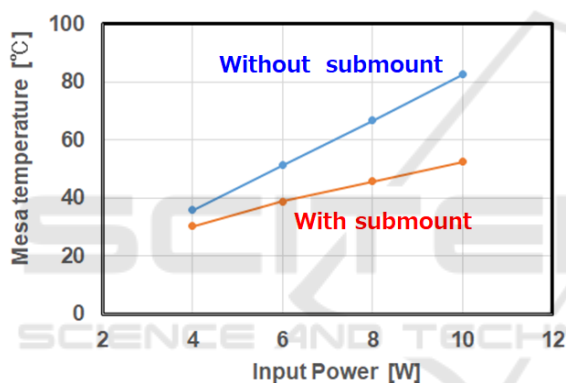


Figure 8: Relationship between input power and temperature rise in the mesa area.

6 DISCUSSION

We discussed the factors that reduce the thermal resistance by using the diamond submount. In the QCL without submount (Fig. 7(a)), the isotherms of the temperature distribution under the mesa are semi-circular, and the heat generated with the input power is transmitted concentrically around the mesa area. On the other hand, in (b), due to the large thermal conductivity of the diamond, the heat spreads horizontally and is transmitted vertically in CuW. To investigate the heat flow in more detail, the heat flux of the surface emission QCL was calculated. Fig. 9(a) shows the distribution of the heat flux vector without submount, and Fig. 9 (b) shows the distribution of the heat flux vector with submount. In Fig. 9(a), the heat flux is mainly directed from the mesa area to the CuW

mount, while in (b) horizontal flux vector is generated in the diamond submount. From the temperature distribution in Fig. 7 and the heat flux distribution in Fig. 9, it is estimated that the heat resistance is reduced by the horizontal transfer of the heat by the diamond submount.

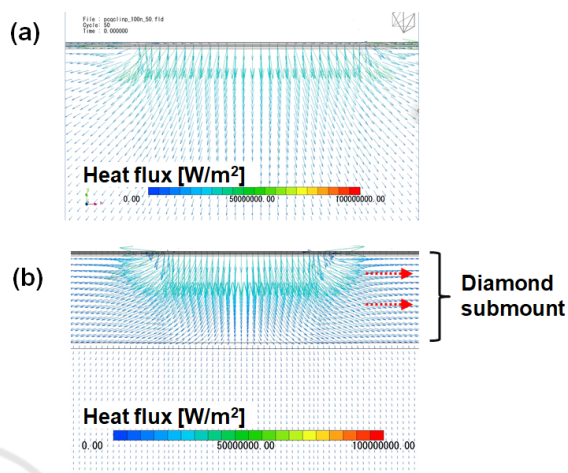


Figure 9: Comparison of heat flux between QCLs with and without diamond submount.

7 CONCLUSIONS

To evaluate the thermal resistance of the InP-embedded surface-emitting QCL, the structure function and 3D thermal analysis simulation were adopted. Using the structure function, the thermal resistance of the surface emitting QCL was divided into the mesa area, the InP substrate, and the CuW mount and the thermal resistance of 8.0 K/W was obtained. The temperature distribution of the surface emission QCL at an input power of 10 W was calculated by the 3D thermal analysis simulation. The thermal resistance obtained from the temperature rise in the mesa area was 8.3 K/W, which was in good agreement with the thermal resistance obtained from the structure function.

Furthermore, the effect of the diamond submount was evaluated by 3D thermal analysis simulation, and it was shown that the thermal resistance was reduced to 5.2 K/W. From the calculation results of the temperature distribution and the heat flux distribution, it was estimated that the heat resistance is reduced by the horizontal transfer of heat by the diamond submount.

ACKNOWLEDGEMENTS

This work was supported by Innovative Science and Technology Initiative for Security (Grant Number JPJ004596), ATLA, Japan.

REFERENCES

- Faist, J., Capasso, F., Sivco, D. L., Sirtori, C., Hutchinson, A., & Cho, A. Y. (1994). Quantum cascade laser. *Science*, 264, 553-556.
- Evans, A., Darvish, S. R., Slivken, S., Nguyen, J., Bai, Y., & Razeghi, M. (2007). Buried heterostructure quantum cascade lasers with high continuous-wave wall plug efficiency. *Appl. Phys. Lett.*, 91, 071101-1-3.
- Colombelli, R., Srinivasan, K., Troccoli, M., Painter, O., Gmachl, C. F., Tennant, D. F., Sergent, A. M., Sivco, D. L., Cho, A. Y., & Capasso, F. (2003). Quantum cascade surface-emitting photonic crystal laser. *Science*, 302, 1374-1377.
- Wang, Z., Liang, Y., Meng, B., Sun, Y-T., Omanakttan, G., Gini, E., Beck, M., Ilija, S., Lourduoss, S., Faist, J., Scalari, G. (2019). Large area photonic crystal quantum cascade laser with 5 W surface-emitting power. *Opt. Express*, 27, 22708-22716.
- Takagi, S., Tanimura, H., Kakuno, T., Hashimoto, R., Saito, S. (2021). Evaluation of thermal resistance of surface-emitting quantum cascade laser using structural function and 3D thermal flow simulation. *PHOTOPTICS2021*, #12.
- Takagi, S., Tanimura, H., Kakuno, T., Hashimoto, R., Saito, S. (2019). Thermal analysis and heat dissipation improvement for quantum cascade lasers through experiments, simulations, and structure function. *Jpn. J. Appl. Phys.*, 58, 091008-1-6.
- Székely, V. (1997). A new evaluation method of thermal transient measurement results. *Microelectron. J.*, 28, 277-292.
- Kim, Y. M., Rodwell, M. J. W., Gossard, A. C. (2002). Thermal characteristics of InP, InAlAs, and AlGaAsSb metamorphic buffer layers used in In_{0.52}Al_{0.48}/In_{0.53}Ga_{0.47}As heterojunction bipolar transistors grown on GaAs substrates. *J. Electron. Mater.*, 31, 196-199.
- Adachi, S. (1985). GaAs, AlAs, and Al_xGa_{1-x}As: Material parameters for use in research and device applications. *J. Appl. Phys.*, 58, R1-R29.
- Bezotosnyi, V. V., Krokhin, O. N., Oleshchenko, V. N., Pevtsov, V.A., Popov, Y. M., Cheshev, E. A. (2014). Thermal modelling of high-power laser diodes mounted using various types of submount. *IEEE J. Quantum Electron.* 44, 899-902.